Forest Ecology and Management 384 (2017) 347–357

Contents lists available at ScienceDirect

Forest Ecology and Management

journal homepage: www.elsevier.com/locate/foreco

Spectral evidence of early-stage spruce beetle infestation in Engelmann spruce

Adrianna C. Foster [a,*], Jonathan A. Walter [b,c], Herman H. Shugart [d], Jason Sibold [e], Jose Negron [f]

[a] University of Virginia, 296 Clark Hall, 291 McCormick Rd., Charlottesville, VA 22904, United States
[b] Virginia Commonwealth University, 1000 W. Cary Street, Richmond, VA 23284, United States
[c] University of Kansas, 2101 Constant Ave., Lawrence, KS 66047, United States
[d] University of Virginia, 376 Clark Hall, 291 McCormick Rd, Charlottesville, VA 22904, United States
[e] Colorado State University, 1787 Campus Delivery, CSU, Fort Collins, CO 80526, United States
[f] USDA Forest Service, Rocky Mountain Research Station, 240 West Prospect, Fort Collins, CO 80526, United States

ARTICLE INFO

Article history:
Received 18 March 2016
Received in revised form 3 November 2016
Accepted 5 November 2016
Available online 15 November 2016

Keywords:
Bark beetle
Hyperspectral
Insect infestation
Landsat
Shortwave infrared
Vegetation stress

ABSTRACT

Spruce beetle (*Dendroctonus rufipennis* (Kirby)) outbreaks cause widespread mortality of Engelmann spruce (*Picea engelmannii* (Parry ex Engelm)) within the subalpine forests of the western United States. Early detection of infestations could allow forest managers to mitigate outbreaks or anticipate a response to tree mortality and the potential effects on ecosystem services of interest. However, the subtle changes in the foliage of infested spruce make early detection difficult. An experiment was conducted in southern Colorado to determine important wavelengths for detecting early-stage (i.e. recently infested) spruce beetle infestation in Engelmann spruce. Spectral reflectance from non-infested and recently infested spruce needles were obtained using the ASDi Field-Spec Pro spectroradiometer. After pre-processing, random forest analysis was used to identify hyperspectral bands and aggregations of hyperspectral bands corresponding to Landsat TM bands and vegetation indices that effectively discriminated between non-infested and infested trees. Results show that the shortwave infrared region of the electromagnetic spectrum was a key area for detecting early stages of spruce beetle infestation, likely due to the effects of beetle infestation on water transport within Engelmann spruce. The strong discriminability of bands in the shortwave infrared region indicates a potential for this spectral region to be used to detect early-stage spruce beetle infestation over larger areas using multispectral satellite imagery. In a preliminary trial, we found that a time series of reflectance in Landsat TM band 7 (shortwave infrared) was strongly correlated with the progression through time of a spruce beetle outbreak in southern Wyoming. These findings suggest that multispectral indicators of early-stage spruce beetle outbreak can be developed. These indicators are needed to better understand spatiotemporal dynamics of spruce beetle outbreaks, and can be used by forest managers to detect early stages of spruce beetle infestation and to potentially mitigate some spruce mortality.

1. Introduction

The spruce beetle (*Dendroctonus rufipennis* (Kirby)) is an important mortality agent of spruce species (*Picea* spp.) throughout the western United States and Canada (Bentz et al., 2010). Within the subalpine forests of the southern Rocky Mountains, its primary host is Engelmann spruce (*Picea engelmannii* (Parry ex Engelm)) (Bebi et al., 2003; Schmid and Frye, 1972). Historically, spruce beetle infestations, along with fire, have been the most important natural disturbances shaping forest structure and function in subalpine forests, and both of these agents are anticipated to increase under a warming climate (Bentz et al., 2010; DeRose and Long, 2012; Hart et al., 2014; Veblen et al., 1991; Westerling et al., 2006). Bark beetle outbreaks have caused widespread tree mortality across the US and Canada in the last several decades, especially in Colorado (Bentz et al., 2009; Berg et al., 2006). In a Colorado outbreak lasting from 1939 to 1952, spruce beetles affected over 290,000 ha of the landscape (Anderson et al., 2010; Veblen et al., 1991), and an ongoing outbreak in Colorado has affected over 638,000 ha between 1996 and 2015 (USFS, 2016). These landscape-scale mortality events modify the size structure and

* Corresponding author.
E-mail addresses: acf7m@virginia.edu (A.C. Foster), jwalter4@vcu.edu (J.A. Walter), hhs@virginia.edu (H.H. Shugart), Jason.Sibold@colostate.edu (J. Sibold), jnegron@fs.fed.us (J. Negron).

http://dx.doi.org/10.1016/j.foreco.2016.11.004
0378-1127/

species composition of forests, especially in terms of basal area, average tree height, and stem density (Derderian et al., 2016; Hawkins et al., 2012; Humphreys and Safranyik, 1993). Biogeochemical cycling in forests is also affected by bark beetle outbreaks, through reduction in stomatal conductance and canopy transpiration (Edburg et al., 2012; Frank et al., 2014), increases in leaf litter and coarse woody debris (Edburg et al., 2012; Meddens et al., 2012), and changes in the carbon balance of the forest (Brown et al., 2012; Edburg et al., 2012; Kurz et al., 2008).

Detection and monitoring of bark beetle outbreaks is crucial to forest management and to deciphering the ecological effects of these organisms. The effects of beetle infestations may be mitigated through various management techniques such as clearing of wind thrown trees, selective thinning, pheromone trapping, and burning (Hansen et al., 2010; Humphreys and Safranyik, 1993; Kautz et al., 2011), especially if these infestations are detected early on in the outbreak cycle (DeRose and Long, 2012; Jenkins et al., 2014). Perhaps more importantly, the relative success of forest treatments as well as the mechanisms and environmental characteristics that lead to outbreaks can be investigated through detection and monitoring of infestation stage and extent (Walter and Platt, 2013).

Aerial detection surveys are often used to assess mortality trends caused by bark beetles (USFS, 2016). Bark beetle-killed trees change in coloration as they desiccate, from green to yellow-green, and with some species to a bright red, and this color change is used as an indicator to map tree mortality. However, this visual detection is not possible in the early (i.e. green) stages of infestation, potentially too late to be helpful for effective management techniques (Franklin et al., 2003). In the case of the closely related mountain pine beetle (*Dendroctonus ponderosae* (Hopkins)), which in the Rocky Mountains infests several *Pinus* species, the foliage of infested trees changes to bright red within one year of being attacked (White et al., 2007). The foliage of spruce beetle-infested Engelmann spruce, however, remains green to yellow-green and photosynthesizing (albeit only slightly) for two or more years after the initial infestation (DeRose et al., 2011; Frank et al., 2014; Schmid, 1976). This several year window of green-stage spruce beetle attack when beetle populations are growing, but detection is difficult, may allow for spruce beetle outbreaks to reach unmanageable levels. Additionally, while aerial surveys are relatively cost-effective for the amount of forest health characteristics that they can provide, and are useful for portraying trends in insect and disease activity, the information is generally at a coarse spatial scale, and may have low positional accuracy (Hall et al., 2016; Wulder et al., 2006c).

In comparison to aerial surveys, remote sensing may allow for more extensive, consistent, and finer-resolution mapping of bark beetle damage, as well as early detection of beetle infestation. To be useful for effective and timely management planning and ecosystem response studies, however, pertinent areas of the electromagnetic spectrum for detecting early-stage spruce beetle infestations must be determined. Many studies have used remote sensing instruments to detect red-stage, and to a lesser extent, green-stage mountain pine beetle outbreaks across a broad range of its hosts, but with varying conclusions on the best waveband or vegetation index to use (Coops et al., 2006a; Franklin et al., 2003; Hall et al., 2016; Meddens and Hicke, 2014; Niemann et al., 2015; Skakun et al., 2003; White et al., 2007, 2005; Wulder et al., 2006a, 2006b). Goodwin et al. (2008) were able to identify red-stage infestation across a large study area (~1.5 million ha) in British Columbia, Canada using Landsat imagery and the normalized difference moisture index (NDMI). Coops et al. (2006a) and Hicke and Logan (2009) both used high spatial resolution QuickBird imagery to accurately map red-attack mountain pine beetle damage using the red-green index (RGI). In contrast, White et al. (2007) found that the moisture stress index (MSI) had the strongest relationship with proportion of red-attack damage using QuickBird and Hyperion imagery.

Much of the success in detecting and monitoring mountain pine beetle outbreaks in broad-scale remote sensors can be attributed to the strong red signature associated with a mountain pine beetle infestation. In contrast, the success of spruce beetle monitoring studies has been more limited. Foliar changes in infested Engelmann spruce are more subtle, and Engelmann spruce typically occurs in mixed spruce-fir stands, unlike generally mono-specific pine stands. The few existing studies on outbreak detection using multispectral remote sensing have been restricted to large-scale outbreaks, or to detecting outbreaks two years or longer into the infestation (DeRose et al., 2011; Frank et al., 2014; Hart and Veblen, 2015; Makoto et al., 2013). DeRose et al. (2011) and Hart and Veblen (2015) utilized multispectral imagery to detect gray-stage spruce beetle infestation with high accuracy using the disturbance index (DI), red-green index (RGI), blue-red index (BR), and normalized difference vegetation index (NDVI). However, spruce trees at the gray stage have already been infested for at least two years (Schmid, 1976), and have started to drop their needles, a point in the outbreak cycle which may be too late for a management response. This difficulty in detecting early-stage spruce beetle infestations suggests a need for higher-sensitivity remote sensors to identify pertinent wavebands for detecting and studying early-stage spruce beetle outbreaks.

Following a spruce beetle infestation, Engelmann spruce close their stomata, resulting in decreased canopy conductance and canopy evapotranspiration (Frank et al., 2014). These and other changes to the foliage of infested spruce may be observable in fine-scale hyperspectral data (Asner et al., 2015; Fassnacht et al., 2014), promising improved algorithms for determining the location and extent of a spruce beetle infestation. Biochemical processes in plants, such as photosynthesis, respiration, and transpiration, are inherently linked to the concentrations of the biochemicals involved in them (Curran et al., 2001). As such, changes initiated by stress, drought, or other factors result in a change in the foliar chemistry of plants. These foliar chemistry changes are often observable in hyperspectral sensors, which detect spectral reflectance in narrow wavebands of the electromagnetic spectrum (Hall et al., 2016; Kokaly and Clark, 1999). Many studies have had success using aerial and ground-based hyperspectral sensors to detect differences in spectral reflectance between leaves with varying pigments, vegetation stress, and bark beetle damage (Carter, 1994; Carter and Knapp, 2001; Delalieux et al., 2009; Fassnacht et al., 2014; Masaitis et al., 2013; Naidu et al., 2009; Santos et al., 2010; Smith et al., 2004). Näsi et al. (2015) used a hyperspectral sensor onboard an unmanned airborne vehicle to detect various stages of European spruce bark beetle (*Ips typographus*) infestation in Norway spruce (*Picea abies* (L. Karst.)). Niemann et al. (2015) and Cheng et al. (2010) both used high spectral resolution sensors to distinguish between healthy and green-stage mountain pine beetle attack, finding the near infrared and shortwave infrared regions to be the most useful. Ahern (1988) also found evidence for detection of green-stage mountain pine beetle infestation using lab spectroscopy, and a study by Carter and Knapp (2001) found significant differences in the 500–700 nm range between lab-derived spectra of healthy and nitrogen-stressed radiata pine (*Pinus radiata* (D. Don)). The success of these studies at using hyperspectral sensors to detect subtle foliar changes due to vegetation stress lends support to the use of hyperspectral data to detect green-stage spruce beetle infestation in Engelmann spruce.

It is clear that hyperspectral remote sensing, with its fine spectral and often fine spatial resolution, can provide detailed biophysical information on canopy properties such as moisture, leaf

nitrogen content, leaf pigment, and tree stress level (Asner et al., 2011; Calderón et al., 2013; Carlson et al., 2007; Kokaly et al., 2009; Underwood et al., 2003). These properties make hyperspectral sensors ideal tools for detecting subtle foliar changes in response to disturbances such as bark beetle infestations. However, the use of aerial and ground-based hyperspectral instruments is expensive and time-consuming, especially when considering large forest landscapes. Multispectral imagery is much more readily available and has a large enough spatiotemporal coverage to monitor yearly or sub-yearly changes in large areas. Thus, freely available broadband imagery is best suited for monitoring whole forest landscapes over time, producing actionable data that forest managers can use to mitigate and predict the spread of insect outbreaks. Yet the low spectral resolution of broadband sensors hinders the process of discovering wavelengths and wavebands important to detecting infestations. These issues present a need for information about such pertinent wavebands to be garnered in local-scale, hyperspectral studies such that they may be scaled up for use in broad-scale monitoring campaigns.

In this study, we use ground-based hyperspectral measurements from the needles of recently infested and non-infested Engelmann spruce to determine areas of the electromagnetic spectrum that could be used to detect early stages of spruce beetle infestation. We use the information garnered from this high spectral and spatial resolution experiment to develop a case for detection of early-stage spruce beetle outbreaks in broad-scale remote sensors (i.e. Landsat, Hyperion, EO-1).

2. Methods

2.1. Study area

This study was conducted at Monarch Pass, a high-elevation site within the spruce-fir (*Picea engelmannii* and *Abies lasiocarpa*) zone of the southern Rocky Mountains (Fig. 1). Monarch Pass (38° 30′ 10.08″N, 106° 20′ 8.1594″; 3442 m) is located in the Sawatch Range of the Rocky Mountains, Grand Mesa-Uncompahgre-Gunnison National Forests, near Salida, CO. This site contains Engelmann spruce trees in various stages of infestation (non-infested, recently infested, and beetle-killed trees). Annual precipitation in the area is 60 cm, and mean monthly temperatures are 14 °C and −5 °C for July and January, respectively (NCDC, 2016).

2.2. Hyperspectral data collection

The ASDi FieldSpec Pro (Analytical Spectral Devices, Inc; Boulder, CO) is a handheld spectroradiometer capable of measuring spectral response over 366 bands, covering wavelengths from 350 to 2500 nm. The spectral resolution of the FieldSpec Pro is 3 nm for wavelengths between 350 and 1000 nm and 10 nm for wavelengths between 1000 and 2500 nm. In order to collect this full wavelength range, the FieldSpec Pro contains three separate spectroradiometers: VNIR (visible and infrared), and SWIR-1 and SWIR-2 (shortwave infrared). Data from this instrument can thus provide information on the spectral properties of leaves in the visible, near infrared, and shortwave infrared regions of the electromagnetic spectrum.

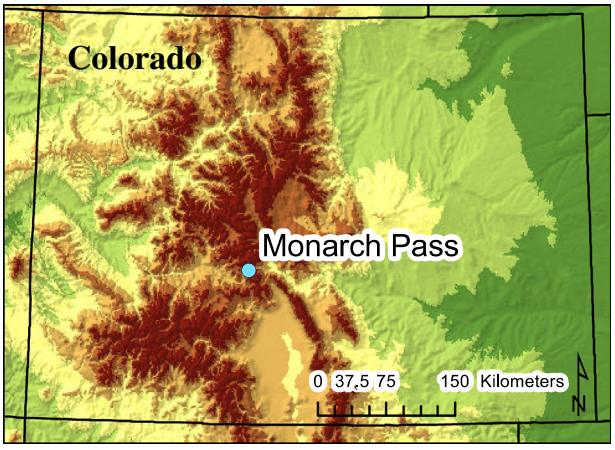

Fig. 1. Location of the study site Monarch Pass in central Colorado.

Engelmann spruce trees were first identified as non-infested or recently infested. Spruce beetles infest their hosts by boring into the bark and laying eggs in the phloem of infested trees (DeRose and Long, 2012). Eggs hatch after a few days and the larvae feed on the tree's phloem. Newly infested trees were identified by the presence of boring dust at bark crevices and the base of the tree, pitch tubes or resin exudation from the bole, and newly constructed egg galleries in the phloem. The flight period when new trees are attacked by spruce beetles reaches its highest point towards the end of July (Negron, unpublished data). As our sampling took place in early September, measurements collected from infested trees took place about 8 weeks after infestation.

Field spectra were collected from 30 spruce trees (15 non-infested, and 15 recently infested) during early September 2014 using the point of contact (POC) method. In this method, the POC probe is placed in direct contact with the sample using a foliage clip, such that no light escapes the POC and no external light is able to affect the sampling. This method uses an internal light source (a quartz-halogen lamp), so sun angle and cloudiness do not affect sampling. Three spectral subsamples were taken from the needles of two branches per tree: one at about 2 m, and a second branch at about 6 m in height (i.e. a total of 90 subsamples for each infestation type). Two branches from each tree were tested to determine if height on the tree had any effect on the spectral signal for spruce beetle infestation. Coloration changes in infested Engelmann spruce trees occur first in the branches of the upper crown (Schmid and Frye, 1977). Because we collected reflectances from branches in the lower canopy, spectral differences between infested and non-infested Engelmann spruce found in this study may be somewhat conservative.

The branches used were clipped from the spruce trees and immediately sampled so as to reduce error associated with being detached from the tree for an extended time period. Each of the three samples per branch was measured using different needles on the branch, and care was taken to only collect spectral signatures from green needles. Each sample involved measuring reflectance of several spruce needles at once. The needles of each sample were arranged on the POC clip so as to maximize the amount of reflected surface area, but minimize overlap and shadowing of needles. Instrument optimization and white reference calibration were conducted after each branch was sampled to correct for atmospheric, temperature, and other changes that may have affected sampling.

2.3. Hyperspectral data processing

First, splice corrections were conducted on all reflectance spectra subsamples. This process reduces discontinuities arising from the three separate detectors (VNIR, SWIR-1, SWIR-2) used to collect the full 350–2500 nm wavelength range. The three subsamples per branch were then averaged. These initial processing methods were all conducted using ViewSpec Pro Software (Analytical Spectral Devices, Inc; Boulder, CO).

Continuum removal was then performed on the 30 branch spectra using ENVI version 5.2 (Exelis Visual Information Solutions; Boulder, CO). Continuum removal reduces spectral changes due

to non-foliar influences such as instrument drift (Kokaly and Clark, 1999). First, a convex hull (or continuum) is fitted over the top of each spectrum that connects local spectral maximums. The continuum-removed reflectance is then calculated by dividing the reflectance values in the original spectrum by the reflectance values of the continuum. This allows for absorption pits to be enhanced and noise due to instrument or other errors to be reduced (Underwood et al., 2003). Finally, it was determined that branch height had no statistical effect on the spectral signals of infested and non-infested trees (see Fig. S1 in the Supplementary Material; $p > 0.05$), so the spectral signatures of high and low branches were averaged for each tree.

2.4. Hyperspectral statistical analyses

In order to determine important wavelengths for differentiating between infested and non-infested trees, a random forest (Breiman, 2001) regression was implemented in R (R Core Team 2014) using the package 'randomForest' (Liaw and Wiener, 2002). Measures of variable importance are an increasingly popular method for variable reduction and for determining which variables best predict the response variable in question (Breiman, 2001; Strobl et al., 2007). In the case of analyzing hyperspectral data, thousands of variables (i.e. reflectance in different wavebands) are collected, and it is imperative that redundant bands are removed and the most important variables for the study at hand are determined (Thenkabail et al., 2012a). The random forest algorithm creates multiple, uncorrelated decision trees using different random subsets of the data and different predictor variables (i.e. different wavelengths). The use of multiple decision trees increases the classification accuracy of the algorithm. Variable importance is then based on the number of times each variable is chosen by different individual decision trees in the random forest and how much each variable contributes to the overall accuracy of the model (Strobl et al., 2007).

Next, the most important wavelengths determined by the random forest were chosen and receiver operator characteristic (ROC) curves were generated on predictions of infested vs. non-infested from classification trees using each of the important variables individually. ROC curves, which plot the rate of true positives against the rate of false positives, can be used to visualize a predictor variable's ability to correctly predict the response variable (i.e. infested or non-infested). The area under the curve (AUC) of an ROC curve represents the probability of the predictor variable accurately choosing the positive case when given a positive and negative test case, and is a widely used test of classification algorithms (Eng, 2005). An AUC of 0.50 is equivalent to random chance. We also generated a confusion matrix (a table for visualization of model performance; Fawcett, 2006) for each wavelength, and from each matrix calculated the overall accuracy, false positive rate, and false negative rate of each wavelength. Next, *t*-tests were conducted to determine if differences between non-infested and infested spruce in spectral reflectance over the eight selected wavelengths were statistically significant. ROC curves, confusion matrices, and *t*-tests were also conducted for several vegetation indices commonly used for vegetation studies and for averages of wavelengths representing Landsat wavebands (Table 1). This was done to determine if an index or a particular waveband in Landsat could also identify early spruce beetle infestation in Engelmann spruce. We chose vegetation indices commonly used to detect bark beetle infestations (Coops et al., 2006a; DeRose et al., 2011; Meddens et al., 2011) as well as those used to detect vegetation stress in general (Calderón et al., 2013; Naidu et al., 2009; Roberts et al., 2012).

3. Results

Much of the average, continuum-removed spectral signatures from infested and non-infested Engelmann spruce overlap (Fig. 2). However, there is divergence in the absorption pit around 1440 nm and across the shortwave infrared region between 1900 and 2480 nm. The spectral reflectance from infested spruce is higher in these regions than that of the non-infested spruce, though this difference is somewhat small (Fig. 3). The random forest regression found several important wavelengths for

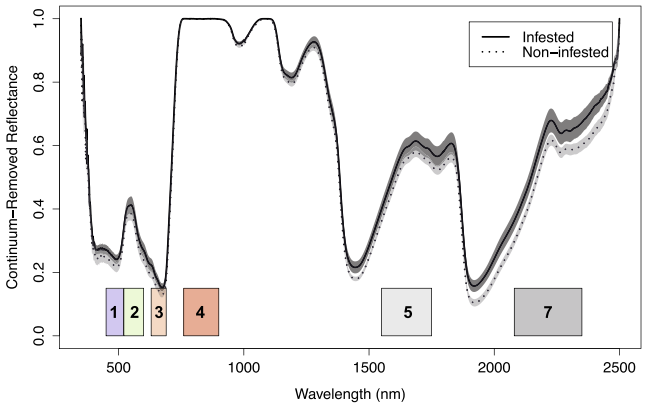

Fig. 2. Average continuum-removed spectral reflectance for infested (solid) and non-infested (dashed) Engelmann spruce trees along with 95% confidence intervals for both spectra (CI = $\bar{x} \pm 2.14SE_{\bar{x}}$). Colored bars represent the wavelength location of Landsat bands. (For interpretation of the references to color in this figure legend, the reader is referred to the web version of this article.)

Table 1
Vegetation indices and Landsat bands used to detect spruce beetle infestation in Engelmann spruce. Blue, green, red, NIR, SWIR1, and SWIR2 were calculated using wavelengths corresponding to Landsat TM bands.

Vegetation index or band name	Equation or wavelength range	Reference
RGI	Red/Green	Coops et al. (2006a)
MCARI	$[(R_{700nm} - R_{670nm}) - 0.2(R_{700nm} - R_{550nm})] * (R_{700nm}/R_{670nm})$	Daughtry et al. (2000)
WI	R_{900nm}/R_{970nm}	Penuelas et al. (1997)
TCWET	Blue * 0.0315 + Green * 2.201 + Red * 0.3102 + NIR * 0.1594 + SWIR1 * 0.6806 − SWIR2 * 0.6109	Crist (1985)
TCGRE	Blue * −0.1603 − Green * 0.281 − Red * 0.4934 − NIR * 0.7940 + SWIR1 * 0.0002 − SWIR2 * 0.1444	Crist (1985)
TCBRI	Blue * 0.2043 + Green * 0.458 + Red * 0.5524 + NIR * 0.5741 + SWIR1 * 0.3124 + SWIR2 * 0.2303	Crist (1985)
DI	TCBRI − TCWET − TCGRE	DeRose et al. (2011)
NDVI	(NIR − Red)/(NIR + Red)	Tucker (1979)
NDMI	(NIR − SWIR1)/(NIR + SWIR1)	Gao (1996)
RVSI	$(R_{714nm} + R_{752nm})/2 - R_{733nm}$	Merton and Huntington (1999)
Landsat band 5	1550–1750 nm	USGS (2016)
Landsat band 7	2080–2350 nm	USGS (2016)

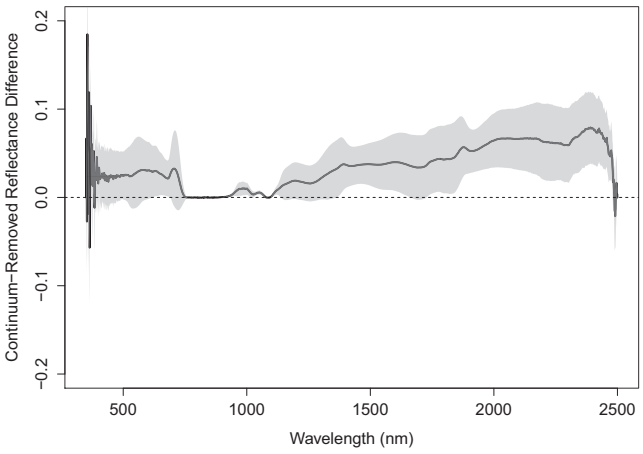

Fig. 3. Average continuum-removed spectral difference between infested and non-infested Engelmann spruce trees (difference = infested − non-infested). Shaded bar represents 95% confidence intervals (CI = $\bar{x} \pm 2.14SE_{\bar{x}}$).

Table 2
Area under the curve (AUC), accuracy, false positive rate, and false negative rate for the eight wavelengths with highest variable importance from the random forest test, and for the vegetation indices and Landsat bands from Table 1 (ordered by accuracy and wavelength). Contingency tables used to calculate error rates can be found in Table S1 in the Supplementary Material.

Wavelengths chosen from random forest test (nm)	AUC	Accuracy	False positives	False negatives
1062	0.93	0.93	0.13	0
1061	0.93	0.93	0.067	0.067
1059	0.93	0.93	0.067	0.067
862	0.93	0.93	0.067	0.067
861	0.93	0.93	0.067	0.067
764	0.93	0.93	0.13	0
368	0.93	0.93	0	0.13
1056	0.9	0.9	0	0.2
VIs and Landsat bands				
Landsat band 7	0.83	0.83	0.26	0.067
NDVI	0.8	0.8	0	0.4
RGI	0.8	0.8	0.3	0.067
WI	0.8	0.8	0.067	0.33
Landsat band 5	0.77	0.77	0.13	0.53
DI	0.77	0.77	0.2	0.267
NDMI	0.77	0.77	0.13	0.33
TCBRI	0.77	0.77	0.067	0.4
TCGRE	0.77	0.77	0	0.467
RVSI	0.67	0.67	0.13	0.53
MCARI	0.63	0.63	0.2	0.53
TCWET	0.63	0.63	0.2	0.53

determining infestation in the Engelmann spruce spectra; most of these are in the far near infrared to shortwave infrared regions (Table 2). We chose the top eight wavelengths to generate classification trees and ROC curves because wavelengths chosen by the random forest algorithm after these eight contributed minimally to overall accuracy. Many of these important wavelengths had high AUC and accuracy values, and low overall error rates (Table 2).

Vegetation indices and averaged Landsat bands derived from the field spectra had lower AUCs and accuracies than did individual hyperspectral bands (Table 2; see Table S1 in the Supplementary Material for contingency matrices). Of these, the red-green index (RGI), water index (WI), NDVI, and Landsat band 7 yielded the highest accuracies. We chose to conduct *t*-tests comparing the reflectance of infested/non-infested samples on the top eight important wavelengths and vegetation indices/Landsat bands with accuracy values above 0.80. The results of these *t*-tests are consistent with the results of the classification trees (Table 3).

Table 3
T-test (n = 30) results for the eight wavelengths with highest variable importance from the random forest test, and the chosen vegetation indices and Landsat band 7. Wavelengths and aggregated indices/wavebands ordered by difference between infested and non-infested spectra.

Wavelengths chosen from random forest (nm)	Difference between infested and non-infested (nm)	t-statistic	p-value
368	0.09513	−4.86	7.11E−05
1056	0.0051	−5.43	5.56E−05
1059	0.00466	−5.28	8.12E−05
1061	0.00433	−5.1614	1.03E−04
1062	0.00411	−5.053	0.00013
861	0.00023	5.91	4.09E−06
862	0.00021	5.98	1.95E−06
764	9E−05	4.7132	1.80E−04
VIs and Landsat bands			
Landsat band 7	0.06435	−3.6487	1.60E−03
RGI	0.03237	−3.031	5.59E−03
NDVI	0.03685	2.8429	8.77E−03
WI	0.011	2.799	1.08E−02

4. Discussion

Early detection of spruce beetle outbreaks may allow forest managers to mitigate an infestation before it turns into a devastating outbreak. A study by DeRose and Long (2012) found evidence for multiple nascent spruce beetle infestations across the study landscape, which the authors posited could only be slowed during the early stages of the outbreak. Once an infestation is identified, managers can potentially reduce the growth rate of spruce beetle populations and limit the severity and extent of growing outbreaks through removal of individual infested trees or downed logs (Hansen et al., 2010). These mitigation techniques would be best applied in areas with high recreational or ecological value and should be applied before infestations reach outbreak levels, during the early, or green stages of beetle infestation. By the time spruce beetle-attacked trees have reached the gray stage, the insects have long since abandoned the tree and initiated new infestations, contributing to the growing outbreak (Schmid and Frye, 1977). Detecting and removing early-stage attacked trees may prevent some of the beetles still within the trees from infesting others, possibly mitigating some mortality. Thus, in order to successfully monitor, manage, and study these important disturbance agents, forest managers and researchers would benefit from an early-stage indicator of spruce beetle infestation. Such an indicator would be made even more useful if it could be applied in sensors with broad spatial coverage and whose data are readily available, such as that of the Landsat series. Until now, remote sensing studies have been focused on detecting gray-stage or later spruce beetle infestations (DeRose et al., 2011; Frank et al., 2014; Hart and Veblen, 2015). This study has the capacity to bridge this knowledge gap and provide insight into what wavebands and indices should be used to detect early-stage spruce beetle infestation.

In this study, we identified several wavelengths and vegetation indices that have potential as indicators of early-stage spruce beetle infestation at the branch and needle level. Of these, several wavelengths in the shortwave infrared region may be most useful (Table 2; Fig. 2). Though reflectances at 368 (ultraviolet) and 764, 861, and 862 (NIR) nm differed between non-infested and infested vegetation and had high overall accuracy values (Tables 2 and 3), the mean differences between infested and non-infested reflectances at these wavelengths, while significant, were quite small. These small differences, manifested in such narrow, specific wavelengths, may be difficult to detect in coarser resolution sensors such as Landsat or QuickBird. These results point to the SWIR region as a better indicator of spruce beetle infestation, especially

as the area of divergence between non-infested and infested spruce in this region overlaps well with multispectral SWIR bands such as Landsat band 7 (Fig. 2).

Overall, the individual chosen hyperspectral wavelengths were better predictors of early-stage spruce beetle infestation than were the vegetation indices/Landsat bands (Table 2). Although we focus on a different stage of infestation, our findings are similar to those of Hart and Veblen (2015), who also found differences between RGI and NDVI for healthy and infested trees. Also in agreement with Hart and Veblen (2015) and DeRose et al. (2011), the disturbance index had a good AUC, at 0.77. However, DI was not the best metric in our case, possibly because we detected green-stage infestation, rather than gray-stage or later. Landsat band 7 also had the lowest error rates of all the calculated indices (Table 2). While commission errors (i.e. false positives) should be avoided, choosing an indicator with a moderate false positive rate, but a low false negative rate would avoid missing infestations altogether.

The higher reflectance of infested spruce in the shortwave infrared region (Fig. 2) can be explained by the underlying physiology of a spruce beetle attack. When a spruce tree is successfully infested by spruce beetles, it receives damage in the form of cambium and phloem consumption by spruce beetle larvae as well as infection with blue-stain fungus, which is vectored by the spruce beetle (Paine et al., 1997; Schmid and Frye, 1977). Frank et al. (2014) found that while canopy conductance of infested Engelmann spruce trees is significantly lower than that of healthy spruce, there is no difference in photosynthesis between rehydrated branches of either class. This suggests that infested spruce trees are tightly regulating their stomatal conductance in response to the hydraulic impacts of the blue stain fungus, while maintaining leaf biochemistry (Frank et al., 2014). Thus, in the early stages of a spruce beetle infestation, Engelmann spruce are slowly losing water due to the decreased canopy conductance, which results in an increase in reflectance in the shortwave infrared region, a primary area for radiation absorption by water (Thenkabail et al., 2012b; Ustin et al., 2004).

A natural extension of these findings would be to evaluate the feasibility of using the wavebands and spectral indices identified in this fine-scale, hyperspectral study as indicators of stand-level early-stage spruce beetle outbreaks in broad-scale imagery, thus providing a more useful and accessible monitoring tool for forest managers. However, several factors complicate extrapolation of these findings. Scaling up from field spectra to broad-scale multispectral imagery such as that of Landsat is complicated by the differences in spectral, spatial, and radiometric resolutions, as well as the differences in the amount of non-foliar reflectance captured in either type of sensor (Coops et al., 2006a; Hall et al., 2016; Lillesand et al., 2000). Of these, non-foliar influences and radiometric resolution are likely to be the least limiting. Non-foliar influences present in broadband pixels can be amended through adequate image selection, classification into vegetated vs. non-vegetated surfaces, and by a number of atmospheric and topographic corrective techniques (Bhandari et al., 2012; Hall et al., 2016; Riano et al., 2003). Additionally, we found fairly strong differences broadly across the SWIR region (Fig. 2); thus radiometric resolution differences between the FieldSpec Pro and broadband satellites are also not likely to be problematic, especially given the high radiometric resolution of newer satellites (e.g. with the 16-bit Landsat OLI).

Decreasing spectral resolution is a large hindrance associated with scaling from hyperspectral to broad-scale sensors (Coops et al., 2006b). Nonetheless, we found evidence for increased reflectance in infested spruce foliage across a broad range of the shortwave infrared region (~1900–2400 nm; Figs. 2 and 3), indicating that multispectral bands in this region (i.e. Landsat band 7) may be useful for detection of early spruce beetle infestation in broadband imagery. The high accuracy and relatively low error rates associated with the averaged Landsat band 7 from the field spectra (Tables 2 and 3) also support its utility in detecting early infestations. We additionally found high accuracy with NDVI and RGI (Table 2), which can also be calculated using broad wavebands (Table 1).

Spatial resolution is also important to consider when conducting vegetation change studies with remote sensing (Coops et al., 2006b; Hall et al., 2016). Sensors with high spatial resolution can detect changes at the scale of single trees or branches, as with the ASDi FieldSpec Pro. However, high spatial resolution typically comes at the expense of low spatial extent and high cost (monetary and time/effort) per unit of information (Coops et al., 2006b; Hall et al., 2016). In our case, the FieldSpec Pro can only sample one branch at a time, and it is not feasible to sample a whole landscape this way. More moderate spatial resolution sensors such as Landsat and Hyperion (each with 30 m pixels) can detect changes at the level of a forest stand (Coops et al., 2006b; Goodwin et al., 2008; Walter and Platt, 2013), cover large areas, and have return times on the order of several days, thereby allowing for identification of stressed stands undergoing early signs of beetle infestation as well as monitoring of infestations through time.

To assess whether the wavelengths identified in our hyperspectral analysis could be used to discriminate spruce beetle infestation in broad-scale multispectral imagery, we conducted a preliminary assessment of Landsat imagery of a recent spruce beetle outbreak in southern Wyoming. The USFS/AmeriFlux site Glacier Lakes Ecosystem Experiments Site (GLEES; in the subalpine zone of the southeastern WY Rocky Mountains) underwent an extensive spruce beetle outbreak between 2005 and 2010 (Frank et al., 2014). Frank et al. (2014) investigated whether they could detect the early stages of this infestation using the MODIS green leaf area product, however, evidence for the outbreak was not observable in MODIS data until about two years after the peak of the outbreak had already occurred. MODIS has a fairly low spatial resolution (250–1000 m) compared to the Landsat series (30 m). Through the use of a finer spatial resolution satellite, and the wavebands identified in our hyperspectral analysis, it is possible that the 2005 spruce beetle outbreak at GLEES may be detectable in Landsat imagery, even in the early stages of the outbreak. If wavelengths identified in our hyperspectral analysis are in fact able to detect infestation at coarser spatial scales and spectral resolutions, this should manifest as coherent changes in corresponding Landsat bands.

We conducted a preliminary case test to begin evaluating the potential for early-stage infestation identification in multispectral satellite imagery. We focused on Landsat band 7 (2080–2350 nm), RGI, and NDVI because of the substantial differences between the foliage of non-infested and infested trees found over these bands and indices in the hyperspectral data. Late summer Landsat 5 TM imagery was used to calculate average rescaled digital number (DN) values for RGI, NDVI, and band 7 for the GLEES outbreak, and these values were plotted across the infestation time series along with data on cumulative percent spruce attacked from Frank et al. (2014) (see Appendix A for more detailed methodology). There was an overall increase in reflectance from Landsat band 7 between 2003 and 2011, coherent with the increase in cumulative attacked spruce with 2010 (Fig. 4). The red-green index had an early peak in 2006 and then seemed to follow reflectance from Landsat band 7, whereas NDVI peaked in 2007 and then decreased. Pearson's correlation coefficients between the attack data and Landsat band 7, RGI, and NDVI are 0.854, 0.690, and −0.485, respectively (see Appendix A for further results).

The coherent changes in the Landsat data record and percent spruce attacked lend support to the idea that stand-level spruce beetle infestation can be detected in broadband imagery, with

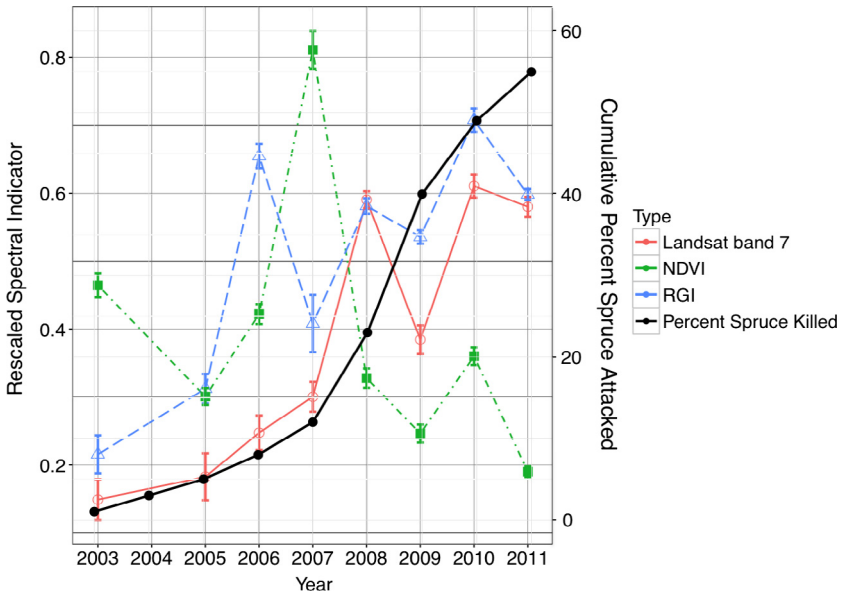

Fig. 4. Average rescaled relative normalized digital number values for Landsat band 7, RGI, and NDVI for forested plots at GLEES during a spruce beetle infestation along with cumulative percent spruce trees attacked redrawn from Frank et al. (2014). Error bars on the spectral indicators represent confidence intervals ($CI = \bar{x} \pm 1.99SE_{\bar{x}}$).

the potential for detection of green-stage outbreaks. Both Landsat band 7, and to some extent RGI, correlated well with the progression of spruce beetle-attacked trees at GLEES (Fig. 4). Band 7 and RGI also increased prior to when this attack could be identified in MODIS data (Frank et al., 2014), and prior to a visual change in the canopy (see photos taken during the infestation in Fig. S2 in Supplementary Material). These increases in RGI and band 7 in the Landsat record prior to visible changes to the canopy further support their utility as green-stage indicators of spruce beetle infestation. Future studies investigating the use of Landsat band 7 and RGI to detect early-stage spruce beetle infestations should include spatially detailed ground truthing at multiple locations and in different times, including all classes of infestation stage. However, the fact that we did see a change in the averaged wavebands and indices, even with the added influence of other infestation classes and other non-foliar influences, lends further support to their use as green-stage indicators of spruce beetle infestation in broadband imagery. Our intent with this preliminary assessment is to bolster the argument for use of information gained at the fine-scale to be used in the more readily available and comprehensive broad-scale satellite record.

The large differences between infested and non-infested spruce in the SWIR region (Fig. 2), relatively high accuracy values of Landsat band 7 and RGI in the hyperspectral data (Table 2), and the early increases in band 7 and RGI in the Landsat imagery at GLEES (Supplemental Fig. S2) implicate the shortwave infrared region and the red-green index as good candidates for detecting early stages of spruce beetle infestation, potentially in broad-scale imagery. This tool would provide managers and other researchers with an easier, more cost-effective way of identifying and potentially mitigating areas of spruce beetle infestation. Many studies have used RGI and the SWIR region to detect vegetation stress due to infestations (Apan et al., 2004; Cheng et al., 2010; Coops et al., 2006a; Delalieux et al., 2007; Hart and Veblen, 2015; Hicke and Logan, 2009; White et al., 2007). Complications with using the SWIR region to detect moisture stress due to early-stage spruce beetle infestations arise from the possibility of misclassifying drought-related stress as a spruce-beetle infestation, or vice versa. Controlling for soil moisture or precipitation using weather or flux tower data could alleviate this problem. However, spruce forests undergoing drought stress are also more likely to be infested by spruce beetles (Berg et al., 2006; Hart et al., 2014; Hebertson and Jenkins, 2008; Malmstrom and Raffa, 2000; McKenzie et al., 2009; Sherriff et al., 2011), and as such detecting spruce forests undergoing drought-related stress may help to identify areas predisposed to infestation.

These findings are an important step towards developing an early-stage detection and monitoring tool for spruce beetle outbreaks, and can serve as the foundation for further studies. Successful monitoring and management of growing spruce beetle outbreaks may help dampen tree mortality and curtail the expansion of infestations. Such monitoring, especially when applied at the early stages of outbreaks, may also provide insight into what climate and environmental factors prompt outbreaks, and what factors influence their spread. Such techniques can be applied locally within the Colorado Rocky Mountains, more broadly across the entire spruce beetle's range, as well as across the ranges of other similar bark beetle species.

5. Conclusions

Under outbreak conditions, spruce beetles can be devastating to the landscape, with consequences ranging from widespread mortality of Engelmann spruce to loss of slope stability and changes in the carbon, water, and energy balances of the forest (Dale et al., 2001; Edburg et al., 2012; Kurz et al., 2008; Veblen et al., 1991). Early detection of spruce beetle infestations would aid in the study of their outbreak dynamics and may help mitigate large-scale outbreaks. Ground-based hyperspectral remote sensing, with its fine spatial and spectral resolution, has been proven to be a valuable tool for understanding the subtle changes in vegetation due to various types of stress and for determining pertinent wavelengths, spectral regions, and vegetation indices useful for classifying healthy and stressed vegetation (Ahern, 1988; Carter, 1993; Delalieux et al., 2007; Santos et al., 2010). The information garnered with such small-scale data can be used to inform studies involving more readily available broadband imagery. We have found, through the use of a ground-based spectroradiometer, that the shortwave infrared region and the red-green index may be useful identifiers of green-stage spruce beetle infestation in

Engelmann spruce. Although we had higher accuracy values for the specific wavelengths of the spectroradiometer than those for the aggregated wavebands or vegetation indices, our findings suggest that these wavebands and indices may also be useful for detecting stand-wide outbreaks using broad-scale multispectral sensors such as Landsat. Our results can be used to inform other studies on detecting and following spruce beetle outbreaks, and perhaps for studies on detecting early-stage infestations from other bark beetles within the Rocky Mountains landscape.

Acknowledgements

This work was funded by the VA Space Grant Consortium Graduate Fellowship (VSGC FY 15-16 to A.C.F., project title "Understanding spruce beetle outbreak dynamics and their response to climate change through remote sensing and ecological modeling") and by a grant from the National Fish and Wildlife Foundation (grant number: 0106.12.032847) to A.C.F. J.A.W. was supported in part by USDA-NIFA 2016-67012-24694. We also thank Sunnie Long for her technical advice and expertise with using the FieldSpec Pro, John Frank and Heather Speckman for use of canopy photography from GLEES, as well as three anonymous reviewers for their very useful comments during the editing and revising of this manuscript.

Appendix A.

A.1. Landsat case test

A.1.1. Study area

The Glacier Lakes Ecosystem Experiments Site (GLEES; Fig. A.1) was used for the case study using Landsat imagery. This separate study area was chosen because (a) Landsat images for relevant years at Monarch Pass were mostly obscured by clouds, and (b) the extent and timing of beetle infestations are documented for GLEES. GLEES experienced a large spruce beetle outbreak between 2005 and 2010 (Frank et al., 2014). GLEES is located in the Snowy Range of the Rocky Mountains in the Medicine Bow-Routt National Forest, near Centennial, WY (41°22′30″N, 106°15′30″W) at elevations ranging from 3200 to 3500 m. The forest is comprised of Engelmann spruce and subalpine fir, with Engelmann spruce dominating the site at 72% of the stems and 84% of the basal area (Frank et al., 2014). Other bark beetles (i.e. *Dendroctonus ponderosae*, *Dryocoetes confuses*) are native to the subalpine zone in this region, however these damage agents were not a significant factor during the period of the spruce beetle outbreak. Average annual precipitation at the site is 100 cm and mean monthly temperatures are 24 °C and −9 °C for July and January, respectively (NRCS, 2014). During the outbreak, rainfall was lower during the beginning stages of the infestation (≈100 cm for 2005 and 2007), and was higher during one of the epidemic years (≈140 cm for 2009) (Frank et al., 2014). Soil moisture was also higher at GLEES during the epidemic years (Frank et al., 2014).

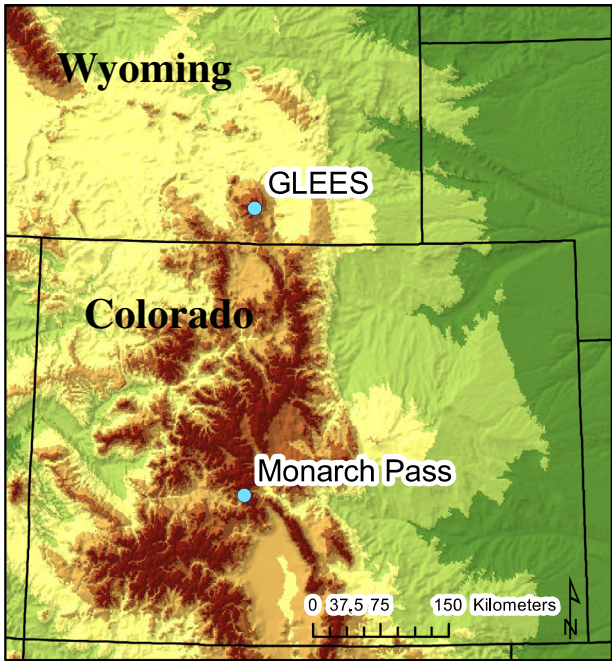

Fig. A.1. Location of the study sites GLEES (southern Wyoming) and Monarch Pass (central Colorado).

A.1.2. Landsat case test methods

Late summer Landsat 5 TM images were obtained over GLEES (path 34, row 31) for 2003, and from 2005 to 2011 (late summer 2004 images were all obscured by clouds). These images span the development of a recent spruce beetle outbreak from endemic (i.e. no infestation or infestation in a small number of isolated, weakened trees), to an epidemic exhibiting high mortality levels, and through the local crash of the outbreak (Frank et al., 2014). The Landsat imagery were clipped to the study area and radiometrically normalized to correct for atmospheric differences between the images. In radiometric normalization, a number of "psuedoinvariant" features are chosen, which are assumed to remain spectrally constant over time (i.e. rocks, roads, lakes, etc.). The reflectances from these surfaces are then used to correct all other scenes for atmospheric or sun/viewing angle differences between the set of images (Yang and Lo, 2000). Radiometric normalization also aids in differentiating change in the imagery due to changes in the spectral properties of the ground surface, and change due simply to noise (Schroeder et al., 2006). Relative radiometric corrections on imagery do not require absolute surface reflectances, as the corrections use only the radiometric information associated with the time series images themselves (Canty and Nielsen, 2008). We used a relative normalization procedure in which image digital numbers (DNs) in 2005–2011 images were linearly related to DNs in the 2003 image using major axis regression. The normalization coefficients were obtained from sets of pseudo-invariant pixels (Schott et al., 1988) and applied to the full images. Radiometric normalization was conducted in R (R Development Core Team 2015) using the package 'landsat' (Goslee, 2011).

The RGI and NDVI were calculated for each image, and the radiometrically calibrated images were then associated with known forest plot locations at GLEES using Geospatial Modelling Environment (Beyer, 2012). Because NDVI and RGI are ratios of digital number (DN) values, whereas the Landsat band 7 response is in digital numbers, the values for these indices were rescaled so that they could be more easily compared. The rescaled relative DN values for Landsat band 7, RGI, and NDVI associated with each plot were averaged by year and plotted over time to determine if change due to beetle infestation was reflected in the Landsat data record, and which (if any) band or index may be a potential indicator for early spruce beetle infestation.

These Landsat data were also plotted along with the spruce beetle attack data from Frank et al. (2014). Frank et al. (2014) calculated cumulative percentage of trees attacked trees using tree cores from a subset of trees at the site. They counted a tree as attacked the year it ceased wood growth, attributing the tree's growth cessation to spruce beetles when accompanied by signs of beetle attack (i.e. pitch tubes). Pearson's product-moment correlation coefficients were calculated to determine the amount

of correlation between the cumulative percent spruce attacked and each vegetation index or band.

A.1.3. Landsat case test results

Landsat band 7 reflectance increased throughout the infestation time series, with a peak in 2010 (Pearson's r = 0.854). The red-green index peaked in 2006, and also increased throughout the infestation (Pearson's r = 0.690). NDVI peaked in 2007, and then decreased throughout the rest of the time series (Pearson's r = −0.485). There was a steady, significant increase in the rescaled relative DN values of band 7 from 2005 to 2007 (p = 0.003 for 2005–2006, p = 0.002 for 2006–2007), which corresponds to the early stages of the spruce beetle outbreak at GLEES, before the peak number of attacks had occurred (Frank et al., 2014). Band 7 was also high in later years, correlating with the epidemic years of the outbreak (2007, 2008, 2010). The decrease in band 7 between 2008 and 2009 may reflect the fact that 2009 was an abnormally wet year, with about 140 cm of rainfall (Frank et al., 2014).

RGI peaked fairly early, in 2006, and was somewhat less correlated with percent attacked spruce than was Landsat band 7 (Pearson's r = 0.690 vs. 0.854). Photos taken by Frank et al. (2014) and Speckman et al. (2015) at the site show that the majority of the canopy was green from 2003 to 2007 (see Fig. S2 in the Supplementary Material). Thus, the increases in RGI and Landsat band 7 occurred before there would have been a strong visual signal for the outbreak. Most of the canopy is green in coloration until after 2007, during which time only about 10% of the forest is infested with spruce beetles, though a significant increase in band 7 and RGI has already occurred.

Because NDVI is a measure of greenness, one would expect NDVI to steadily decrease as the infestation progressed. However, this was not the case; NDVI over GLEES increased until 2007, after which it did in fact decrease. In images from GLEES (Fig. S2; Supplementary Material) one can see that in 2009, and especially 2010, many yellow and gray spruce trees can be seen, which may account for the drop in NDVI.

Appendix B. Supplementary material

Supplementary data associated with this article can be found, in the online version, at http://dx.doi.org/10.1016/j.foreco.2016.11.004.

References

Ahern, F., 1988. Effects of bark beetle stress on the foliar spectral reflectance of lodgepole pine. Int. J. Remote Sens. 9, 1451–1468.

Anderson, R.S., Smith, S.J., Lynch, A.M., Geils, B.W., 2010. The pollen record of a 20th century spruce beetle (*Dendroctonus rufipennis*) outbreak in a Colorado subalpine forest, USA. For. Ecol. Manage. 260, 448–455. http://dx.doi.org/10.1016/j.foreco.2010.05.001.

Apan, A., Held, A., Phinn, S., Markley, J., 2004. Detecting sugarcane "orange rust" disease using EO-1 Hyperion hyperspectral imagery. Int. J. Remote Sens. 25. http://dx.doi.org/10.1080/01431160310001618031.

Asner, G., Martin, E.M., Kapp, D.E., Tupayachi, R., Anderson, C., Carranza, L., Martinez, P., Houcheime, M., Sinca, F., Weiss, P., 2011. Spectroscopy of canopy chemicals in humid tropical forests. Remote Sens. Environ. 115, 3587–3598.

Asner, G.P., Martin, R.E., Anderson, C.B., Knapp, D.E., 2015. Quantifying forest canopy traits: imaging spectroscopy versus field survey. Remote Sens. Environ. 158, 15–27.

Bebi, P., Kulakowski, D., Veblen, T.T., 2003. Interactions between fire and spruce beetles in a subalpine Rocky Mountain forest landscape. Ecology 84, 362–371.

Bentz, B., Logan, J., MacMahon, J., Allen, C.D., Ayres, M., Berg, E., Carroll, A., Hansen, M., Hicke, J., Joyce, L., et al., 2009. Bark Beetle Outbreaks in Western North America: Causes and Consequences. Bark Beetle Symposium, Snowbird Utah.

Bentz, B.J., Régnière, J., Fettig, C.J., Hansen, E.M., Hayes, J.L., Hicke, J.A., Kelsey, R.G., Negrón, J.F., Seybold, S.J., 2010. Climate change and bark beetles of the western United States and Canada: direct and indirect effects. Bioscience 60, 602–613. http://dx.doi.org/10.1525/bio.2010.60.8.6.

Berg, E.E., Henry, J.D., Fastie, C.L., De Volder, A.D., Matsuoka, S.M., 2006. Spruce beetle outbreaks on the Kenai Peninsula, Alaska, and Kluane National Park and Reserve, Yukon Territory: relationship to summer temperatures and regional differences in disturbance regimes. For. Ecol. Manage. 227, 219–232.

Beyer, H.L., 2012. Geospatial Modeling Environment.

Bhandari, S., Phinn, S., Gill, T., 2012. Preparing Landsat image time series (LITS) for monitoring changes in vegetation phenology in Queensland, Australia. Remote Sens. 4, 1856–1886.

Breiman, L., 2001. Random forests. Mach. Learn. 45, 5–32.

Brown, M.G., Black, T.A., Nesic, Z., Fredeen, A.L., Foord, V.N., Spittlehouse, D.L., Bowler, R., Burton, P.J., Trofymow, J.A., Grant, N.J., Lessard, D., 2012. The carbon balance of two lodgepole pine stands recovering from mountain pine beetle attack in British Columbia. Agric. For. Meteorol. 153, 82–93. http://dx.doi.org/10.1016/j.agrformet.2011.07.010.

Calderón, R., Navas-Cortés, J.A., Lucena, C., Zarco-Tejada, P.J., 2013. High-resolution airborne hyperspectral and thermal imagery for early detection of Verticillium wilt of olive using fluorescence, temperature and narrow-band spectral indices. Remote Sens. Environ. 139, 231–245. http://dx.doi.org/10.1016/j.rse.2013.07.031.

Canty, M.J., Nielsen, A.A., 2008. Automatic radiometric normalization of multitemporal satellite imagery with the iteratively re-weighted MAD transformation. Remote Sens. Environ. 112, 1025–1036.

Carlson, K.M., Asner, G.P., Hughes, R.F., Ostertag, R., Martin, R.E., 2007. Hyperspectral remote sensing of canopy biodiversity in Hawaiian lowland rainforests. Ecosystems 10, 536–549. http://dx.doi.org/10.1007/s10021-007-9041-z.

Carter, G.A., 1993. Responses of leaf spectral reflectance to plant stress. Am. J. Bot. 80, 239. http://dx.doi.org/10.2307/2445346.

Carter, G.A., 1994. Ratios of leaf reflectances in narrow wavebands as indicators of plant stress. Int. J. Remote Sens. 15, 697–703.

Carter, G.A., Knapp, A.K., 2001. Leaf optical properties in higher plants: linking spectral characteristics to stress and chlorophyll concentration. Am. J. Bot. 88, 677–684.

Cheng, T., Rivard, B., Sanchez-Azofeifa, G.A., Feng, J., Calvo-Polanco, M., 2010. Continuous wavelet analysis for the detection of green attack damage due to mountain pine beetle infestation. Remote Sens. Environ. 114, 899–910.

Coops, N.C., Johnson, M., Wulder, M.A., White, J.C., 2006a. Assessment of QuickBird high spatial resolution imagery to detect red attack damage due to mountain pine beetle infestation. Remote Sens. Environ. 103, 67–80.

Coops, N.C., Wulder, M.A., White, J.C., 2006b. Identifying and describing forest disturbance and spatial pattern: data selection issues and methodological implications. In: Wulder, M.A., Franklin, S.E. (Eds.), Understanding Forest Disturbance and Spatial Pattern: Remote Sensing and GIS Approaches. Taylor & Francis, pp. 31–61.

Crist, E.P., 1985. A TM tasseled cap equivalent transformation for reflectance factor data. Remote Sens. Environ. 17, 301–306.

Curran, P.J., Dungan, J., Peterson, D.L., 2001. Estimating the foliar biochemical concentration of leaves with reflectance spectrometry: testing the Kokaly and Clark methodologies. Remote Sens. Environ. 76, 349–359.

Dale, V.H., Joyce, L.A., Mcnulty, S., Neilson, R.P., Ayres, M.P., Flannigan, M.D., Hanson, P.J., Irland, L.C., Lugo, A.E., Peterson, C.J., Simberloff, D., Swanson, F.J., Stocks, B.J., Michael Wotton, B., 2001. Climate change and forest disturbances. Bioscience 51, 723. http://dx.doi.org/10.1641/0006-3568(2001)051[0723:CCAFD]2.0.CO;2.

Daughtry, C.S.T., Walthall, C.L., Kim, M.S., Brown de Colstoun, E., McMurtrey III, J.E., 2000. Estimating corn leaf chlorophyll concentration from leaf and canopy reflectance. Remote Sens. Environ. 74, 229–239.

Delalieux, S., Van Aardt, J., Keulemans, W., Schrevens, E., Coppin, P., 2007. Detection of biotic stress (*Venturia inaequalis*) in apple trees using hyperspectral data: non-parametric statistical approaches and physiological implications. Eur. J. Agron. 27, 130–143.

Delalieux, S., Somers, B., Verstraeten, W.W., van Aardt, J.A.N., Keulmans, W., Coppin, P., 2009. Hyperspectral indices to diagnose leaf biotic stress of apple plants, considering leaf phenology. Int. J. Remote Sens. 30. http://dx.doi.org/10.1080/01431160802541556.

Derderian, D., Dang, H., Aplet, G.H., Binkley, D., 2016. Bark beetle effects on a seven-century chronosequence of Engelmann spruce and subalpine fir in Colorado, USA. For. Ecol. Manage. 361, 154–162.

DeRose, R.J., Long, J.N., 2012. Factors influencing the spatial and temporal dynamics of Engelmann spruce mortality during a spruce beetle outbreak on the Markagunt Plateau, Utah. For. Sci. 58, 1–14. http://dx.doi.org/10.5849/forsci.10-079.

DeRose, R.J., Long, J.N., Ramsey, R.D., 2011. Combining dendrochronological data and the disturbance index to assess Engelmann spruce mortality caused by a spruce beetle outbreak in southern Utah, USA. Remote Sens. Environ. 115, 2342–2349. http://dx.doi.org/10.1016/j.rse.2011.04.034.

Edburg, S.L., Hicke, J.A., Brooks, P.D., Pendall, E.G., Ewers, B.E., Norton, U., Gochis, D., Gutmann, E.D., Meddens, A.J., 2012. Cascading impacts of bark beetle-caused tree mortality on coupled biogeophysical and biogeochemical processes. Front. Ecol. Environ. 10, 416–424. http://dx.doi.org/10.1890/110173.

Eng, J., 2005. Receiver operating characteristic analysis: a primer. Acad. Radiol. 12, 909–916.

Fassnacht, F.E., Latifi, H., Ghosh, A., Joshi, P.K., Koch, B., 2014. Assessing the potential of hyperspectral imagery to map bark beetle-induced tree mortality. Remote Sens. Environ. 140, 533–548. http://dx.doi.org/10.1016/j.rse.2013.09.014.

Fawcett, T., 2006. An introduction to ROC analysis. Pattern Recognit. Lett. 27, 861–874.

Frank, J.M., Massman, W.J., Ewers, B.E., Huckaby, L.S., Negrón, J.F., 2014. Ecosystem CO_2/H_2O fluxes are explained by hydraulically limited gas exchange during tree mortality from spruce bark beetles: CO_2/H_2O flux explained from disturbance. J.

Geophys. Res. Biogeosci. 119, 1195–1215. http://dx.doi.org/10.1002/2013JG002597.
Franklin, S.E., Wulder, M.A., Skakun, R.S., Carroll, A.L., 2003. Mountain pine beetle red-attack forest damage classification using stratified Landsat TM data in British Columbia, Canada. Photogramm. Eng. Remote Sens. 69, 283–288.
Gao, B., 1996. NDWI-A normalized difference water index for remote sensing of vegetation liquid water from space. Remote Sens. Environ. 58, 257–266.
Goodwin, N.R., Coops, N.C., Wulder, M.A., Gillanders, S., Schroeder, T., Nelson, T., 2008. Estimation of insect infestation dynamics using a temporal sequence of Landsat data. Remote Sens. Environ. 112, 3680–3689.
Goslee, S.C., 2011. Analyzing remote sensing data in R: the landsat package. J. Stat. Softw. 43, 1–25.
Hall, R.J., Castilla, G., White, J.C., Cooke, B.J., Skakun, R.S., 2016. Remote sensing of forest pest damage: a review and lessons learned from a Canadian perspective. Can. Entomol. http://dx.doi.org/10.4039/tce.2016.11.
Hansen, E.M., Negron, J.F., Munson, A.S., Anhold, J.A., 2010. A retrospective assessment of partial cutting to reduce spruce beetle-caused mortality in the southern Rocky Mountains. West. J. Appl. For. 25, 81–87.
Hart, S.J., Veblen, T.T., 2015. Detection of spruce beetle-induced tree mortality using high- and medium-resolution remotely sensed imagery. Remote Sens. Environ. 168, 134–145. http://dx.doi.org/10.1016/j.rse.2015.06.015.
Hart, S.J., Veblen, T.T., Eisenhart, K.S., Jarvis, D., Kulakowski, D., 2014. Drought induces spruce beetle (*Dendroctonus rufipennis*) outbreaks across northwestern Colorado. Ecology 95, 930–939.
Hawkins, C.D.B., Dhar, A., Balliet, N.A., Runzer, K.D., 2012. Residual mature trees and secondary stand structure after mountain pine beetle attack in central British Columbia. For. Ecol. Manage. 277, 107–115. http://dx.doi.org/10.1016/j.foreco.2012.04.023.
Hebertson, E.G., Jenkins, M.J., 2008. Climate factors associated with historic spruce beetle (Coleoptera: Curculionidae) outbreaks in Utah and Colorado. Environ. Entomol. 37, 281–292.
Hicke, J.A., Logan, J., 2009. Mapping whitebark pine mortality caused by a mountain pine beetle outbreak with high spatial resolution satellite imagery. Int. J. Remote Sens. 30, 4427–4441.
Humphreys, N., Safranyik, L., 1993. Spruce beetle (No. Foret Pest Leaflet 13). Natural Resources Canada, Pacific Forestry Centre, Victoria, B.C.
Jenkins, M.J., Hebertson, E.G., Munson, A.S., 2014. Spruce beetle biology, ecology, and management in the Rocky Mountains: an addendum to Spruce Beetles in the Rockies. Forests 5, 21–71.
Kautz, M., Dworschak, K., Gruppe, A., Schopf, R., 2011. Quantifying spatio-temporal dispersion of bark beetle infestations in epidemic and non-epidemic conditions. For. Ecol. Manage. 262, 598–608.
Kokaly, R.F., Clark, R.N., 1999. Spectroscopic determination of leaf biochemistry using band-depth analysis of absorption features and stepwise multiple linear regression. Remote Sens. Environ. 67, 267–287.
Kokaly, R.F., Asner, G.P., Ollinger, S.V., Martin, M.E., Wessman, C.A., 2009. Characterizing canopy biochemistry from imaging spectroscopy and its application to ecosystem studies. Remote Sens. Environ. 113, S78–S91.
Kurz, W.A., Dymond, C.C., Stinson, G., Rampley, G.J., Neilson, E.T., Carroll, A.L., Ebata, T., Safranyik, L., 2008. Mountain pine beetle and forest carbon feedback to climate change. Nature 452, 987–990. http://dx.doi.org/10.1038/nature06777.
Liaw, A., Wiener, M., 2002. Classification and regression by randomForest. R News 2, 18–22.
Lillesand, T.M., Kiefer, R.W., Chipman, J., 2000. Remote Sensing and Image Analysis. Wiley, New York, NY.
Makoto, K., Tani, H., Kamata, N., 2013. High-resolution multispectral satellite image and a postfire ground survey reveal prefire beetle damage on snags in Southern Alaska. Scand. J. For. Res. 28, 581–585.
Malmstrom, C.M., Raffa, K.F., 2000. Biotic disturbance agents in the boreal forest: considerations for vegetation change models. Glob. Change Biol. 6, 35–48.
Masaitis, G., Mozgeris, G., Augustaitis, A., 2013. Spectral reflectance properties of healthy and stressed coniferous trees. IForest – Biogeosciences For. 6, 30–36. http://dx.doi.org/10.3832/ifor0709-006.
McKenzie, D., Peterson, D.L., Littell, J.J., 2009. Chapter 15 global warming and stress complexes in forests of Western North America. In: Developments in Environmental Science. Elsevier, pp. 319–337.
Meddens, A.J.H., Hicke, J.A., 2014. Spatial and temporal patterns of Landsat-based detection of tree mortality caused by mountain pine beetle outbreak in Colorado, USA. For. Ecol. Manage. 322, 78–88.
Meddens, A.J.H., Hicke, J., Ferguson, C.A., 2011. Evaluating the potential of multispectral imagery to map multiple stages of tree mortality. Remote Sens. Environ. 115, 1632–1642.
Meddens, A.J., Hicke, J.A., Ferguson, C.A., 2012. Spatiotemporal patterns of observed bark beetle-caused tree mortality in British Columbia and the western United States. Ecol. Appl. 22, 1876–1891.
Merton, R., Huntington, J., 1999. Early simulation results of the ARIES-1 satellite sensor for multi-temporal vegetation research derived from AVIRIS. In: Proceedings of the Eighth Annual JPL Airborne Earth Science Workshop. Pasadena, CA: NASA, JPL, p. 1999.
Naidu, R.A., Perry, E.M., Pierce, F.J., Mekuria, T., 2009. The potential of spectral reflectance technique for the detection of Grapevine leafroll-associated virus-3 in two red-berried wine grape cultivars. Comput. Electron. Agric. 66, 38–45. http://dx.doi.org/10.1016/j.compag.2008.11.007.
Näsi, R., Honkavaara, E., Lyytikäinen-Saarenmaa, P., Blomqvist, M., Litkey, P., Hakala, T., Viljanen, N., Kantola, T., Tanhuanpää, T., Holopainen, M., 2015. Using UAV-based photogrammetry and hyperspectral imaging for mapping bark beetle damage at tree-level. Remote Sens. 7, 15467–15493.
NCDC, 2016. Monthly Climatological Summary, Saint Elmo, CO US GHCND: USS0006L05S.
Niemann, K.O., Quinn, G., Visintini, F., Parton, D., 2015. Hyperspectral remote sensing of mountain pine beetle with an emphasis on previsual assessment. Can. J. Remote Sens. 41, 191–202.
NRCS, 2014. Natural Resources Conservation Service, National Water and Climate Center: SNOTEL Site Brooklyn Lake [WWW Document]. URL <http://www.wcc.nrcs.usda.gov/nwcc/site?sitenum=367>.
Paine, T.D., Raffa, K.F., Harrington, T.C., 1997. Interactions among Scolytid bark beetles, their associated fungi, and live host conifers. Annu. Rev. Entomol. 42, 179–206.
Penuelas, J., Pinol, J., Ogaya, R., Fillella, I., 1997. Estimation of plant water concentration by the reflectance Water Index WI (R900/R970). Int. J. Remote Sens. 18. http://dx.doi.org/10.1080/014311697217396.
Riano, D., Chuvieco, E., Salas, J., Aguado, I., 2003. Assessment of different topographic corrections in Landsat-TM data for mapping vegetation types. IEEE Trans. Geosci. Remote Sens. 41, 1056–1061.
Roberts, D.A., Roth, K.L., Perroy, R.L., 2012. Hyperspectral vegetation indices. In: Thenkabail, P.S., Lyon, J.G., Huete, A. (Eds.), Hyperspectral Remote Sensing of Vegetation. CRC Press: Taylor & Francis Group, Boca Raton, FL, pp. 309–328.
Santos, M.J., Greenberg, J.A., Ustin, S.L., 2010. Using hyperspectral remote sensing to detect and quantify southeastern pine senescence effects in red-cockaded woodpecker (*Picoides borealis*) habitat. Remote Sens. Environ. 114, 1242–1250.
Schmid, J.M., 1976. Temperatures, growth, and fall of needles on Engelmann spruce infested by spruce beetles. (Forest Service Research Note No. RM-331). USDA.
Schmid, J.M., Frye, R.H., 1972. Biological evaluation of spruce beetle mortality, Wolf Creek Pass, CO (USDA Forest Service, Rocky Mountain Forest and Range Experiment Station No. Unumbered Report). Fort Collins, CO.
Schmid, J.M., Frye, R.H., 1977. Spruce Beetle in the Rockies.
Schott, J., Salvaggio, C., Volchok, W., 1988. Radiometric scene normalization using pseudoinvariant features. Remote Sens. Environ. 26, 1–16.
Schroeder, T.A., Cohen, W.B., Song, C., Canty, M.J., Yang, Z., 2006. Radiometric correction of multi-temporal Landsat data for characterization of early successional forest patterns in western Oregon. Remote Sens. Environ. 103, 16–26.
Sherriff, R.L., Berg, E.E., Miller, A.E., 2011. Climate variability and spruce beetle (*Dendroctonus rufipennis*) outbreaks in south-central and southwest Alaska. Ecology 92, 1459–1470.
Skakun, R.S., Wulder, M.A., Franklin, S.E., 2003. Sensitivity of the thematic mapper enhanced wetness difference index to detect mountain pine beetle red-attack damage. Remote Sens. Environ. 86, 433–443. http://dx.doi.org/10.1016/S0034-4257(03)00112-3.
Smith, K.L., Steven, M.D., Colls, J.J., 2004. Use of hyperspectral derivative ratios in the red-edge region to identify plant stress response to gas leaks. Remote Sens. Environ. 92, 207–217.
Speckman, H.N., Frank, J.M., Bradford, J.B., Miles, B.L., Massman, W.J., Parton, W.J., Ryan, M.G., 2015. Forest ecosystem respiration estimated from eddy covariance and chamber measurements under high turbulence and substantial tree mortality from bark beetles. Glob. Change Biol. 21, 708–721.
Strobl, C., Boulesteix, A.L., Hothorn, T., 2007. Bias in random forest variable importance measures: Illustrations, sources and a solution. BMC Bioinformatics 8. http://dx.doi.org/10.1186/1471-2105-8-25.
Thenkabail, P.S., Lyon, J.G., Huete, A., 2012a. Advances in hyperspectral remote sensing of vegetation and agricultural croplands. In: Press, C.R.C. (Ed.), Hyperspectral Remote Sensing of Vegetation. Taylor & Francis Group, pp. 3–35.
Thenkabail, P.S., Lyon, J.G., Huete, A., 2012b. Hyperspectral remote sensing of vegetation and agricultural crops: knowledge gain and knowledge gap after 40 years of research. In: Thenkabail, P.S., Lyon, J.G., Huete, A. (Eds.), Hyperspectral Remote Sensing of Vegetation. CRC Press: Taylor & Francis Group, Boca Raton, FL, pp. 663–688.
Tucker, C.J., 1979. Red and photographic infrared linear combinations for monitoring vegetation. Remote Sens. Environ. 8, 127–150.
Underwood, E., Ustin, S., DiPietro, D.B., 2003. Mapping nonnative plants using hyperspectral imagery. Remote Sens. Environ. 86, 150–161.
USFS, 2016. Aerial Survey Highlights for Colorado 2015 [WWW Document]. URL <http://www.fs.usda.gov/detail/r2/forest-grasslandhealth/?cid=fseprd489834>.
USGS, 2016. Frequently Asked Questions About the Landsat Missions [WWW Document]. USGS Landsat Missions, URL. <http://landsat.usgs.gov/band_designations_landsat_satellites.php>.
Ustin, S.L., Roberts, D.A., Gamon, J.A., Asner, G.P., Green, R.O., 2004. Using imaging spectroscopy to study ecosystem processes and properties. Bioscience 54, 523–534.
Veblen, T.T., Hadley, K.S., Reid, M.S., Rebertus, A.J., 1991. The response of subalpine forests to spruce beetle outbreak in Colorado. Ecology 72, 213. http://dx.doi.org/10.2307/1938916.
Walter, J.A., Platt, R.V., 2013. Multi-temporal analysis reveals that predictors of mountain pine beetle infestation change during outbreak cycles. For. Ecol. Manage. 302, 308–318. http://dx.doi.org/10.1016/j.foreco.2013.03.038.
Westerling, R.J., Hidalgo, H.G., Cayan, D.R., Swetnam, T.W., 2006. Warmer and earlier spring increases western US forest wildfire activity. Science 313, 940–943.
White, J.C., Wulder, M.A., Brooks, D., Reich, R., Wheate, R.D., 2005. Detection of red attack stage mountain pine beetle infestation with high spatial resolution satellite imagery. Remote Sens. Environ. 96, 340–351.

White, J.C., Coops, N.C., Hilker, T., Wulder, M.A., Carroll, A.L., 2007. Detecting mountain pine beetle red attack damage with EO-1 Hyperion moisture indices. Int. J. Remote Sens. 28, 2111–2121.

Wulder, M.A., Dymond, C.C., White, J.C., Leckie, D.G., Carroll, A.L., 2006a. Surveying mountain pine beetle damage of forests: a review of remote sensing opportunities. For. Ecol. Manage. 221, 27–41.

Wulder, M.A., White, J.C., Bentz, B., Alvarez, M.F., Coops, N.C., 2006b. Estimating the probability of mountain pine beetle red-attack damage. Remote Sens. Environ. 101, 150–166. http://dx.doi.org/10.1016/j.rse.2005.12.010.

Wulder, M.A., White, J.C., Bentz, B.J., Ebata, T., 2006c. Augmenting the existing survey hierarchy for mountain pine beetle red-attack damage with satellite remotely sensed data. For. Chron. 82, 187–202.

Yang, X., Lo, C.P., 2000. Relative radiometric normalization performance for change detection from multi-date satellite images. Photogramm. Eng. Remote Sens. 66, 967–980.